

Computational design of a renewable organic reagent for photochemical reduction of CO₂ with visible light

Barry K. Carpenter* and Ian Rose

Physical Organic Chemistry Centre, Cardiff University, Cardiff CF10 3AT, UK

Email: carpenterb1@cardiff.ac.uk

Dedicated to Professor Keith Smith on the occasion of his 65th birthday

Abstract

Density functional calculations have been used to design an organic molecule that should be capable of reducing carbon dioxide to formic acid, using the energy from visible light. The compound combines the functions of photocatalyst and reducing agent, and is designed to be renewable by hydrogenation of its oxidation product. The keys to the design are the photochemical generation of a zwitterion in a form that is kinetically inhibited from return to the ground state, and the reduction of CO₂ by direct hydride addition rather than separate electron and proton additions.

Keywords: CO₂ reduction, photochemistry, density functional theory

Introduction

The topic of artificial photosynthesis has received considerable renewed interest in recent years, because it is seen as one way in which the energy from sunlight might be stored in chemical form.¹ However, direct photosynthesis – simultaneous photochemical reduction of CO₂ and oxidation of water – is very difficult to accomplish, because these redox transformations are individually challenging and the optimum conditions for their accomplishment are often mutually incompatible. By most estimates, even the highly evolved photosynthetic systems of plants typically accomplish photosynthesis with <5% efficiency in the use of the incident light energy.²

Work from this laboratory has recently demonstrated the feasibility of an alternative strategy to the simultaneous reduction and oxidation reactions.³ It involves the use of a renewable reducing agent for photochemical reduction of CO₂. The regeneration of the reducing agent involves hydrogenation. If the hydrogen for this step were to have come from one of the increasingly efficient methods of photochemical water splitting,⁴ then the net effect would be artificial photosynthesis, but with the oxidation and reduction steps conducted separately. This

strategy allows optimum conditions for the redox reactions to be employed without needing to worry about their compatibility. It also divides the thermodynamic burden of the overall photosynthetic transformation into separate pieces, making them more readily achievable with visible photons.³

In the prototype for the new strategy, we used a photocatalyst whose absorption maximum was in the UV.⁵ Ultimately, such a photocatalyst will not be optimal if one wants to harness solar radiation as the energy source, because the maximum in the sea level solar irradiance spectrum occurs near 600 nm. We have obtained preliminary results showing that the same reducing agent will work with rhenium catalysts operating in the visible region.⁶ However this strategy has its own set of problems. In particular, it is now widely recognized that chemistry relying on the use of very rare elements, such as rhenium, will never be economically viable for use on very large scale.⁷ Consequently, if the strategy that we have developed is to have any prospects for further development, it must be modified so that the chemistry can be accomplished with visible light and with reagents containing only Earth-abundant elements. The calculations reported in this paper have been undertaken with the purpose of designing such reagents.

Results and Discussion

One strategy for designing a reagent with the properties outlined in the introduction would be to ascertain whether the transition metal complexes that are currently successful for visible-light reduction of CO₂ could be modified to use only Earth-abundant metals, such as iron. However, we have adopted an alternative approach, which avoids the use of transition metals altogether; the reagent that we propose would be purely organic. One reason for this choice is that our earlier successful prototype was designed after extensive initial computational work, and electronic structure models are, to date, much more reliable for organic molecules than for transition metal complexes, especially when it comes to photochemistry.⁸ We have adopted a similar strategy for the current task, and it is the results of the calculations that are presented here.

Having made the choice to focus on organic reagents, one faces an immediate problem having to do with the wavelength of light that can be used. Almost all existing methods for photochemical reduction of CO₂ are believed to begin with the addition of an electron, generating CO₂^{•-}.⁹ The known organic photocatalysts that can accomplish this difficult step all operate with UV light.⁵ The success of transition metal complexes in achieving the chemistry with visible light apparently arises from their ability to bind CO₂^{•-} to the metal, thereby making the reduction more favorable and reducing the energy of the photons required to drive it.¹⁰ It is not at all obvious how one would adopt a similar strategy in an organic system. For this reason, we chose to explore an alternative approach, which would avoid the generation of CO₂^{•-} altogether. This could be accomplished, in principle, by hydride addition to CO₂ – in effect making the reduction thermodynamically more favorable than the alternative electron + H atom

addition by an amount equal to the difference in the C–H bond dissociation enthalpy of formate anion and the electron affinity of H^{\bullet} .

The design principle that we have explored for the photochemical preparation of a hydride donor involves the generation of a kinetically trapped zwitterion. As described below, the kinetic trap is intended to inhibit the return of the zwitterion to the ground state. The molecule is trapped by a double intersystem crossing, from initially excited singlet state to a triplet biradical and from there back to the singlet manifold, but in a conformation that generates and kinetically isolates the reactive zwitterion.

The molecule selected to realize all of these requirements is substituted naphthalene **1**, shown in Figure 1.

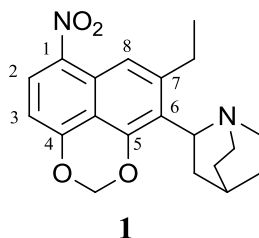
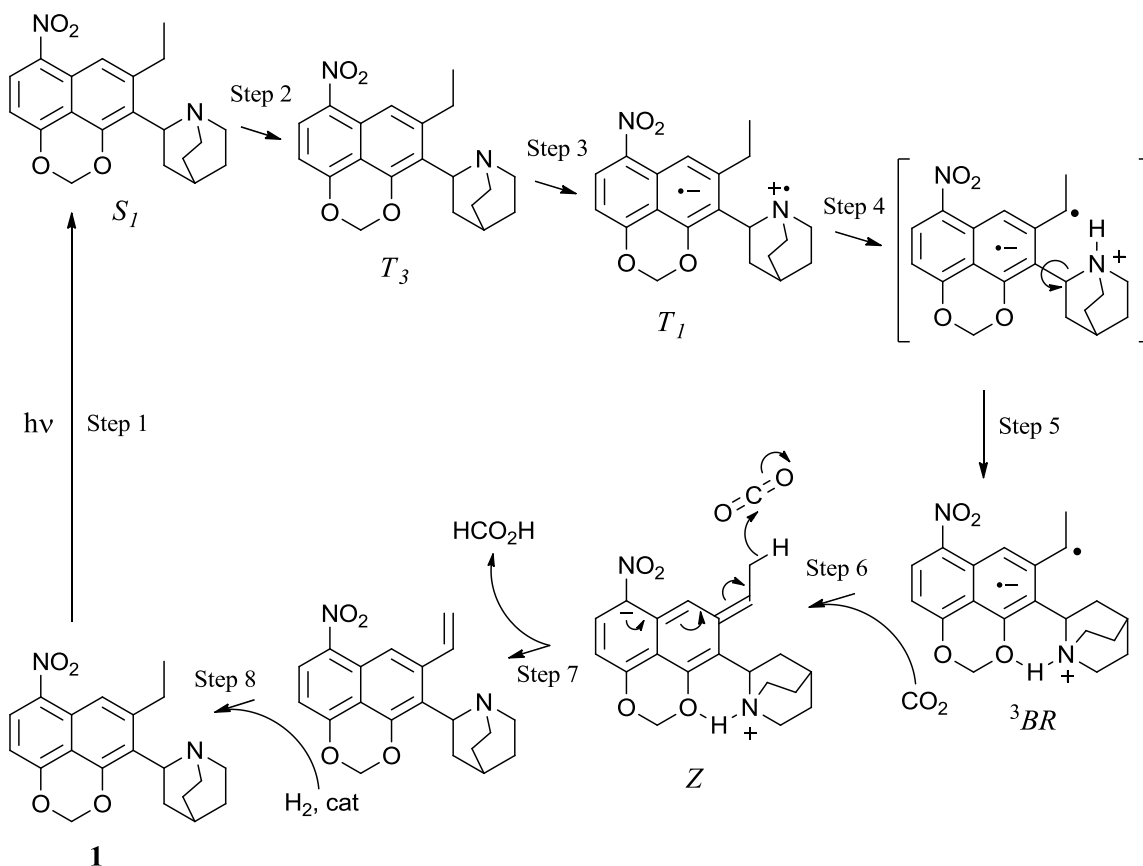


Figure 1. The molecule designed to act as a renewable photoreductant for CO_2 .

The various components of this molecule have the following purposes.

1. The 1-nitronaphthalene base structure is designed to take advantage of the ultrafast intersystem crossing from S_1 to T_3 which molecules of this class are known to exhibit.¹¹
2. The quinuclidine attached to C6 is designed to quench the T_1 state by intramolecular electron transfer¹² and then to abstract a hydrogen atom from the methylene of the ethyl group on C7. The bicyclic structure of the tertiary amine moiety is designed to inhibit proton or hydrogen atom loss from the corresponding radical cation.³
3. The ethyl group on C7 is intended to be the source of a hydride and then, indirectly, a proton for the conversion of CO_2 to formic acid.
4. The methylenedioxy group spanning C4 and C5 has three purposes. Firstly, it extends the λ_{max} for the (π,π^*) absorption of compound **1** into the visible region of the spectrum. Secondly, the oxygen on C5 acts as a hydrogen bond acceptor in the zwitterionic tautomer of **1** (*vide infra*), providing the kinetic barrier against its return to the starting state. Third, it provides a regiochemical control element for the intended synthetic route to **1**, which involves an intramolecular cycloaddition.

The ways in which these component parts of the design come together to achieve the intended goal are summarized in Scheme 1.



Scheme 1. Summary of the proposed reaction steps leading to CO₂ reduction and then regeneration of compound **1**.

Most of the steps in Scheme 1 have been analyzed for their energetic viability by density functional theory (DFT) calculations. The remainder of this section provides the details of what we have found.

Step 1. The UV-visible spectrum of compound **1** was predicted on the basis of time-dependent (TD) density functional theory,¹³ in combination with an integral-equation formulation of the polarizable-continuum (IEFPCM) solvent model.¹⁴ Specifically, the geometry of **1** was optimized at the B3LYP/6-31+G(d), and then a single-point TD-B3LYP/6-31+G(d) calculation carried out with IEFPCM simulation of acetonitrile solvent. The result is shown in Figure 2. Although the absorption maximum is not predicted to be coincident with the maximum in the solar irradiance spectrum, it is definitely in the visible region. If the general strategy outlined here proves to be successful experimentally, modification of the photoreductant to move its absorption maximum to longer wavelength would probably be feasible.

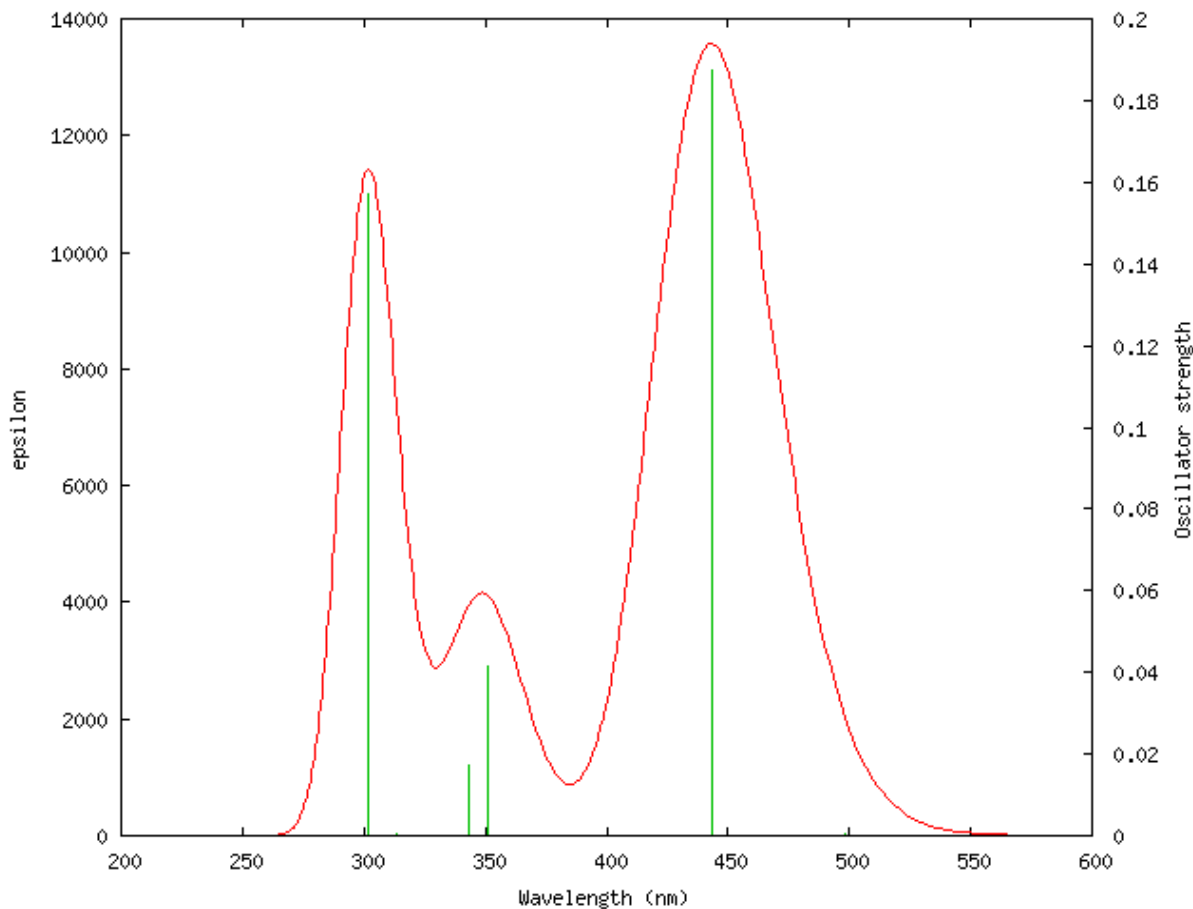


Figure 2. Computed UV-visible spectrum of compound **1** in acetonitrile solution.

Steps 2 and 3. The DFT computational model employed in the present work is not capable of describing higher excited states, and so the T_3 state implicated in Scheme 1 has not been subjected to direct calculation. Its inclusion in the Scheme is based on very extensive experimental precedent, showing ultrafast intersystem crossing ($k_{ISC} \sim 10^{13} \text{ s}^{-1}$) from S_1 to T_3 not only in 1-nitronaphthalene itself, but also in a variety of analogs.¹¹ Decay to T_1 in these systems has typically been found to occur on the 10-100 ps timescale.¹¹

The quenching of nitronaphthalene T_1 by bicyclic amines, such as DABCO, is also well preceded experimentally.¹² In the prior studies, this electron-transfer reaction occurred intermolecularly, but in the present case it would be an intramolecular event. That raises the question of whether T_1 is already the charge-transfer state. According to our B3LYP calculations it is not, because the computed spin density on the amine nitrogen is very low (0.00475). However, it is known that B3LYP can have difficulty in representing excited charge-transfer states,¹⁵ and so how well this result mirrors reality is unknown.

Step 4. The intramolecular H-atom transfer in the T_1 state is the direct analog of the H-atom transfer that formed the foundation for our successful prototype of a renewable reducing agent

for CO₂.³ It occurs in the six-membered-ring transition state that is invariably the most favorable for such reactions,¹⁶ and is computed to have a classical Gibbs energy barrier of only 4 kcal/mol. Any contribution from tunneling would presumably make the effective barrier even smaller. The computed molecular structure for the transition state is shown in Figure 3.

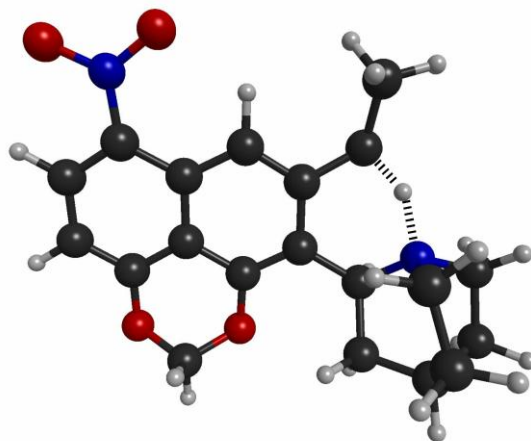
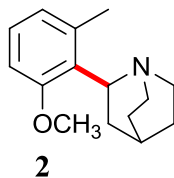


Figure 3. Computed transition structure for intramolecular H-atom transfer in the T₁ state of compound **1**.

Step 5. A crucial design principle for our system is that C → N hydrogen transfer be exergonic in the T₁ state but endergonic in the Z state (see Scheme 1 for state labels). This combination allows the generation of a reactive intermediate with sufficiently high free energy to effect CO₂ reduction. However, for that strategy to work, the Z state must be protected from the intramolecular back transfer of the N–H, which would simply return it unprofitably to the starting state. The device selected for this purpose is the generation of a strong intramolecular hydrogen bond. The idea behind this was explored thoroughly with the model compound **2**. A complete, relaxed potential energy profile was calculated for internal rotation about the C–C bond of compound **2** that is highlighted in red. This calculation was conducted for both neutral **2** and its conjugate acid (protonated on nitrogen). The results are summarized in Figure 4.



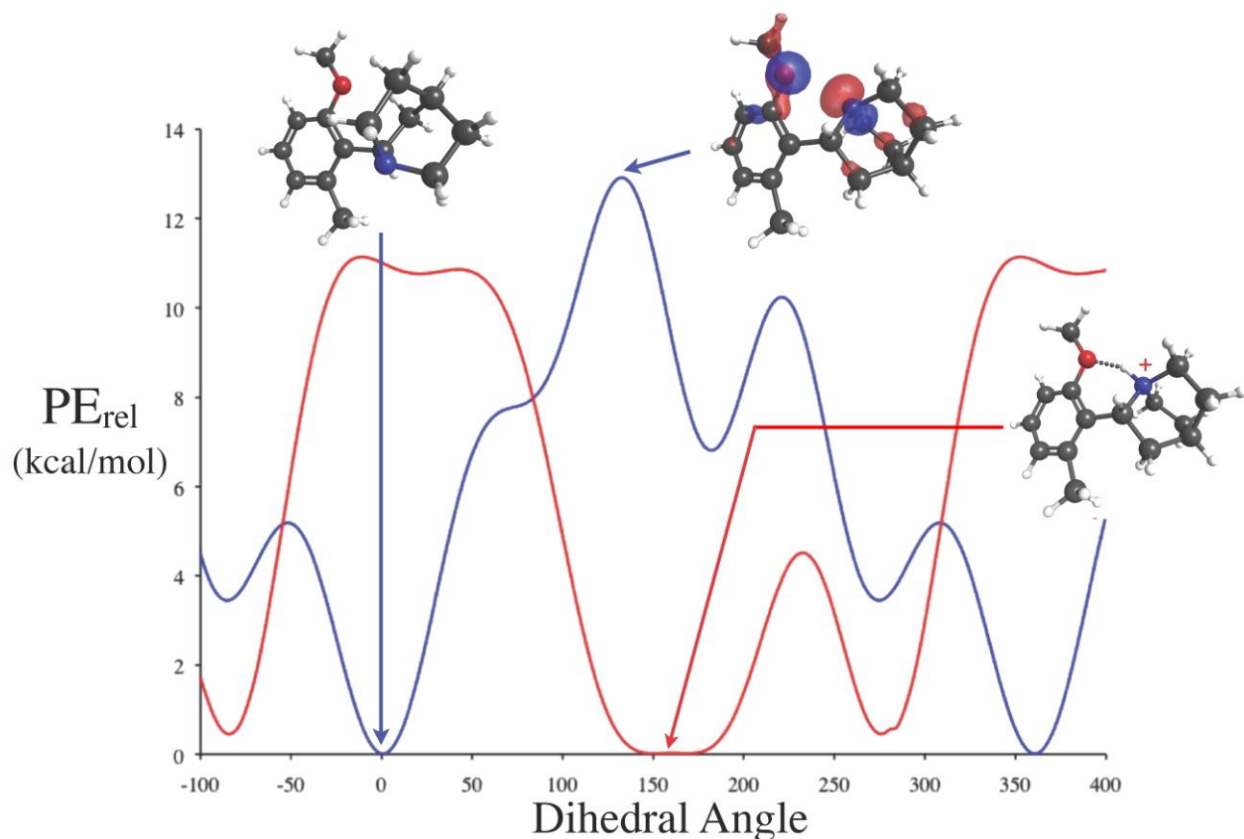


Figure 4. B3LYP/6-31+G(d) relaxed PE profiles for internal rotation about the highlighted C–C bond of compound **2** and its conjugate acid. The blue curve is for neutral **2** and the red curve for the N-protonated form.

For neutral **2**, the calculations reveal a PE minimum (used to define the zero dihedral angle) corresponding to a rotamer in which the quinuclidine nitrogen and the aryl methyl group are proximate to each other. For compound **1** this would be the conformation necessary to allow the intramolecular H-atom transfer described in Step 4. The PE maximum corresponds to a close approach of the nitrogen and oxygen atoms of compound **2**, and is presumably attributable to repulsion between the lone pairs on these atoms (shown in Figure 4). Protonation of the nitrogen leads to a dramatic change, in which the previous PE minimum at a dihedral angle of 0° becomes a maximum, whereas the previous maximum at $\sim 150^\circ$ becomes a minimum. This is clearly attributable to the formation of a strong hydrogen bond between protonated nitrogen and oxygen. According to the calculations, the H-bond is worth about 11 kcal/mol.

The implication for compound **1** is that completion of the H-atom transfer in Step 4 of the mechanism should be followed by an essentially barrierless internal rotation to generate the intramolecular hydrogen bond between the protonated nitrogen and the oxygen on C5 of the naphthalene. And, indeed, that is what the calculations find: the minimum energy geometry for the triplet biradical has this geometry, with the hydrogen bond in place.

Step 6. This is the crucial step for the whole scheme, because it generates the intermediate capable of hydride donation to CO₂. The step begins with intersystem crossing back into the singlet manifold. According to the DFT calculations, this is thermodynamically favorable by 13.5 kcal/mol (Gibbs energy). The result is the zwitterion, Z, which is kinetically inhibited from returning to **1** by the hydrogen bond discussed above. The transition state for hydride transfer from Z to CO₂ enjoys a stabilizing interaction that was not anticipated in the original design. As shown in Figure 5, the computed transition structure reveals that an oxygen of the partially reduced CO₂ is apparently more basic than the C5 oxygen of the methylenedioxy moiety, because it now acts as the H-bond acceptor for the protonated nitrogen:

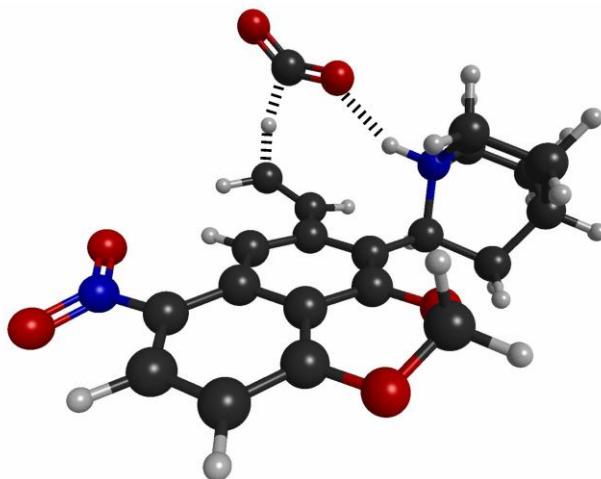


Figure 5. Calculated transition structure for the reduction of CO₂ by zwitterion Z.

The computed Gibbs energy of activation for the CO₂ reduction by Z is 12 kcal/mol with respect to a 1M standard state at 298 K. This is very close to the computed barrier to internal rotation, which would return Z to the starting state, **1**. If these numbers were accurate, then there would obviously be a competition between these two processes, favoring the CO₂ reduction at higher CO₂ concentration (for example, in supercritical CO₂), but the likely error in DFT calculations of the type used here is sufficiently high that it does not seem worthwhile to speculate about this in detail. Elucidation of the real situation will have to wait for the experiments.

Step 7. This step is simply the catalytic hydrogenation that regenerates compound **1** from its dehydrogenated derivate. No calculations were carried out on this step.

Conclusions

The calculations reported here suggest that it should be possible to design an organic compound that would serve as both photocatalyst and reducing agent for the reduction of CO₂, using visible light. In addition, the reagent could be regenerated by hydrogenation after use. If the hydrogen used for that purpose were generated by photochemical water splitting,⁴ the net result would be to couple photochemical reduction of CO₂ and oxidation of water, thereby creating an artificial photosynthetic system.

The particular compound studied in the present work is just a starting point. It is almost inevitable that complications not anticipated in these calculations will arise when this scheme is reduced to practice. Nonetheless, the cycle of computational exploration followed by experimental refinement, which led to a successful design of the first renewable photochemically activated reducing agent for CO₂, has now been initiated for this second-generation reagent. The next step is to synthesize and test compound **1**.

Computational Details

Because these calculations represent just the first step in a cycle of theoretical and experimental study, and because there is every reason to believe that reduction to practice will reveal the need for modifications of the prototype, it was judged to be prudent at this stage to use a computational model that would give credible results, but not to invest the resources necessary to achieve the highest possible accuracy (which would require explicit solvent models and the use of methods capable of describing both dispersion effects and charge-transfer excited states accurately). With this pragmatic philosophy in mind, the calculations used the B3LYP hybrid density functional model, as implemented in the Gaussian 03 computational package.¹⁷ Geometry optimizations of stationary points (minima and transition structures) in Scheme 1 were carried out with a 6-31+G(d,p) basis set and included the IEFPCM solvent simulation for acetonitrile during the optimization and subsequent vibrational frequency calculations. Computed Gibbs energies were referred to a standard state of 1M.

Acknowledgements

All calculations were performed using the computational facilities of the Advanced Research Computing @ Cardiff (ARCCA) Division, Cardiff University. Support of this work by the Leverhulme Trust is gratefully acknowledged.

References

1. Amao, Y. *Chemcatchem* **2011**, *3*, 458.
2. Blankenship, R. E.; Tiede, D. M.; Barber, J.; Brudvig, G. W.; Fleming, G.; Ghirardi, M.; Gunner, M. R.; Junge, W.; Kramer, D. M.; Melis, A.; Moore, T. A.; Moser, C. C.; Nocera, D. G.; Nozik, A. J.; Ort, D. R.; Parson, W. W.; Prince, R. C.; Sayre, R. T. *Science* **2011**, *332*, 805.
3. Richardson, R. D.; Holland, E. J.; Carpenter, B. K. *Nature Chem.* **2011**, *3*, 301.
4. Reece, S. Y.; Hamel, J. A.; Sung, K.; Jarvi, T. D.; Esswein, A. J.; Pijpers, J. J. H.; Nocera, D. G. *Science* **2011**, *334*, 645.
5. Matsuoka, S.; Kohzuki, T.; Pac, C.; Ishida, A.; Takamuku, S.; Kusaba, M.; Nakashima, N.; Yanagida, S. *J. Phys. Chem.* **1992**, *96*, 4437.
6. Takeda, H.; Koike, K.; Inoue, H.; Ishitani, O. *J. Am. Chem. Soc.* **2008**, *130*, 2023.
7. Du, P. W.; Eisenberg, R. *Energy & Env. Sci.* **2012**, *5*, 6012.
8. Gonzalez, L.; Escudero, D.; Serrano-Andres, L. *Chemphyschem* **2012**, *13*, 28.
9. Shkrob, I. A.; Dimitrijevic, N. M.; Marin, T. W.; He, H. Y.; Zapol, P. *J. Phys. Chem. C* **2012**, *116*, 9461.
10. Agarwal, J.; Johnson, R. P.; Li, G. H. *J. Phys. Chem. A* **2011**, *115*, 2877.
11. Plaza-Medina, E. F.; Rodriguez-Cordoba, W.; Peon, J. *J. Phys. Chem. A* **2011**, *115*, 9782.
12. Gerner, H.; Dopp, D. *J. Chem. Soc., Perkin Trans. 2* **2002**, 120.
13. Stratmann, R. E.; Scuseria, G. E.; Frisch, M. J. *J. Chem. Phys.* **1998**, *109*, 8218.
14. Cancès, E.; Mennucci, B.; Tomasi, J. *J. Chem. Phys.* **1997**, *107*, 3032.
15. Dreuw, A.; Weisman, J. L.; Head-Gordon, M. *J. Chem. Phys.* **2003**, *119*, 2943.
16. Pfaendtner, J.; Yu, X. R.; Broadbelt, L. J. *J. Phys. Chem. A* **2006**, *110*, 10863.
17. Gaussian 03, Revision C.02, Frisch, M. J.; Trucks, G. W.; Schlegel, H. B.; Scuseria, G. E.; Robb, M. A.; Cheeseman, J. R.; Montgomery, Jr., J. A.; Vreven, T.; Kudin, K. N.; Burant, J. C.; Millam, J. M.; Iyengar, S. S.; Tomasi, J.; Barone, V.; Mennucci, B.; Cossi, M.; Scalmani, G.; Rega, N.; Petersson, G. A.; Nakatsuji, H.; Hada, M.; Ehara, M.; Toyota, K.; Fukuda, R.; Hasegawa, J.; Ishida, M.; Nakajima, T.; Honda, Y.; Kitao, O.; Nakai, H.; Klene, M.; Li, X.; Knox, J. E.; Hratchian, H. P.; Cross, J. B.; Bakken, V.; Adamo, C.; Jaramillo, J.; Gomperts, R.; Stratmann, R. E.; Yazyev, O.; Austin, A. J.; Cammi, R.; Pomelli, C.; Ochterski, J. W.; Ayala, P. Y.; Morokuma, K.; Voth, G. A.; Salvador, P.; Dannenberg, J. J.; Zakrzewski, V. G.; Dapprich, S.; Daniels, A. D.; Strain, M. C.; Farkas, O.; Malick, D. K.; Rabuck, A. D.; Raghavachari, K.; Foresman, J. B.; Ortiz, J. V.; Cui, Q.; Baboul, A. G.; Clifford, S.; Cioslowski, J.; Stefanov, B. B.; Liu, G.; Liashenko, A.; Piskorz, P.; Komaromi, I.; Martin, R. L.; Fox, D. J.; Keith, T.; Al-Laham, M. A.; Peng, C. Y.; Nanayakkara, A.; Challacombe, M.; Gill, P. M. W.; Johnson, B.; Chen, W.; Wong, M. W.; Gonzalez, C.; and Pople, J. A.; Gaussian, Inc., Wallingford CT, 2004.